

# Transcriptional profiling of lung cell populations in idiopathic pulmonary arterial hypertension

Didem Saygin<sup>1</sup> , Tracy Tabib<sup>2</sup>, Humberto E.T. Bittar<sup>3</sup>, Eleanor Valenzi<sup>4</sup>, John Sembrat<sup>4</sup>, Stephen Y. Chan<sup>4</sup>, Mauricio Rojas<sup>4</sup> and Robert Lafyatis<sup>2</sup>

<sup>1</sup>Department of Medicine, University of Pittsburgh Medical Center, Pittsburgh, PA, USA; <sup>2</sup>Division of Rheumatology, Department of Medicine, University of Pittsburgh Medical Center, Pittsburgh, PA, USA; <sup>3</sup>Department of Pathology, University of Pittsburgh Medical Center, Pittsburgh, PA, USA; <sup>4</sup>Division of Cardiology, Department of Medicine, University of Pittsburgh Medical Center, Pittsburgh, PA, USA

## Abstract

Despite recent improvements in management of idiopathic pulmonary arterial hypertension, mortality remains high. Understanding the alterations in the transcriptome–phenotype of the key lung cells involved could provide insight into the drivers of pathogenesis. In this study, we examined differential gene expression of cell types implicated in idiopathic pulmonary arterial hypertension from lung explants of patients with idiopathic pulmonary arterial hypertension compared to control lungs. After tissue digestion, we analyzed all cells from three idiopathic pulmonary arterial hypertension and six control lungs using droplet-based single cell RNA-sequencing. After dimensional reduction by t-stochastic neighbor embedding, we compared the transcriptomes of endothelial cells, pericyte/smooth muscle cells, fibroblasts, and macrophage clusters, examining differential gene expression and pathways implicated by analysis of Gene Ontology Enrichment. We found that endothelial cells and pericyte/smooth muscle cells had the most differentially expressed gene profile compared to other cell types. Top differentially upregulated genes in endothelial cells included novel genes: *ROBO4*, *APCDD1*, *NDST1*, *MMRN2*, *NOTCH4*, and *DOCK6*, as well as previously reported genes: *ENG*, *ORAI2*, *TFDPI*, *KDR*, *AMOTL2*, *PDGFB*, *FGFR1*, *EDNI*, and *NOTCH1*. Several transcription factors were also found to be upregulated in idiopathic pulmonary arterial hypertension endothelial cells including *SOX18*, *STRA13*, *LYL1*, and *ELK*, which have known roles in regulating endothelial cell phenotype. In particular, *SOX18* was implicated through bioinformatics analyses in regulating the idiopathic pulmonary arterial hypertension endothelial cell transcriptome. Furthermore, idiopathic pulmonary arterial hypertension endothelial cells upregulated expression of *FAM60A* and *HDAC7*, potentially affecting epigenetic changes in idiopathic pulmonary arterial hypertension endothelial cells. Pericyte/smooth muscle cells expressed genes implicated in regulation of cellular apoptosis and extracellular matrix organization, and several ligands for genes showing increased expression in endothelial cells. In conclusion, our study represents the first detailed look at the transcriptomic landscape across idiopathic pulmonary arterial hypertension lung cells and provides robust insight into alterations that occur in vivo in idiopathic pulmonary arterial hypertension lungs.

## Keywords

pulmonary arterial hypertension, single cell RNA-sequencing, endothelial cells, pericytes

Date received: 30 November 2019; accepted: 29 January 2020

Pulmonary Circulation 2020; 10(1) 1–15

DOI: 10.1177/2045894020908782

## Introduction

Idiopathic pulmonary arterial hypertension (IPAH) is a disease characterized by excessive pulmonary vasoconstriction and pathologic remodeling of small pulmonary arterioles. These changes, in turn, lead to increased intravascular pressures in lung and right ventricular dysfunction. Advances in understanding of IPAH pathogenesis in the last 25 years has

led to development of targeted therapies and associated improvement in survival rates in IPAH.<sup>1</sup> These current targeted treatments include prostacyclin analogs that increase

Corresponding author:

Robert Lafyatis, 200 Lothrop Street, BST S720, Pittsburgh, PA 15260, USA.

Email: lafyatis@pitt.edu



deficient prostacyclin, endothelin receptor antagonists that inhibit endothelin pathway and phosphodiesterase-5 inhibitors, as well as soluble guanylyl cyclase agonists that augment nitric oxide signaling. However, despite recent improvements in management, IPAH remains a devastating disease.<sup>2</sup> Therefore, understanding IPAH pathogenesis is critical to facilitate development of novel approaches to therapy in the near future.

The pulmonary vascular wall consists of a single layer of endothelial cells (ECs) in the innermost layer, surrounded by pericytes and vascular smooth muscle cells, and extracellular matrix and fibroblasts in the adventitial layer. Pathogenesis of IPAH involves complex interaction between these different cell types. Reduced vessel diameter and increased vascular stiffness are hallmark features, and result from inflammation, proliferation, contraction, thrombosis, and pathological vascular remodeling of pulmonary vessels. EC dysfunction is regarded to play a major role and is characterized by imbalance between production of vasoconstrictors (thromboxane, endothelin, serotonin) versus vasodilators (nitric oxide, prostacyclin, vasoactive intestinal peptide), promoting (fibroblast growth factor-2) versus inhibiting vascular smooth muscle cell proliferation and recruitment of inflammatory cells versus anti-inflammatory effects.<sup>3,4</sup> Vascular smooth muscle cell proliferation and contraction occurs as a result of activation of hypoxia-inducible factor-1 alpha (HIF1 $\alpha$ ), downregulation of potassium channels, and upregulation of transient receptor potential channels and anti-apoptotic proteins.<sup>5</sup> Roles of ECs and vascular smooth muscle cells in IPAH pathogenesis are relatively well-recognized compared to other cell types such as pericytes, fibroblasts, dendritic cells, and lymphoid cells. However, in addition to the defined roles of individual cell types, there is also growing evidence that ECs and pericytes acquire mesenchymal phenotypes similar to vascular smooth muscle cells and play further propagating role in vascular remodeling.<sup>6</sup>

Given dynamic changes in the roles and type of the cells, understanding the transcriptome–phenotype of each lung cell type could shed light on IPAH pathobiology. Previous methodologies used for gene expression analyses are limited by their inability to examine discrete cell types in complex tissues. Single-cell RNA sequencing (scRNA-seq) is a state of art technique that enables analysis of the transcriptomic-phenotype of each of the cell types simultaneously in a tissue. In this study, we sought to define differential gene expression of lung cells in IPAH compared to controls, using scRNA-seq technology.

## Methods

### Study participants

The University of Pittsburgh Medical Center Institutional Review Board (Pittsburgh, PA, USA) reviewed and approved the conduct of this study. Human sample

procurement was consistent with the Declaration of Helsinki. Normal and IPAH lungs were obtained under a protocol approved by the University of Pittsburgh. Normal lungs were obtained following rejection as candidate donors for transplant, while IPAH lungs were obtained following removal of recipients' lungs during transplantation surgery. Pulmonary hypertension was defined hemodynamically as mean pulmonary arterial pressure  $\geq 25$  mmHg, pulmonary arterial wedge pressure  $\leq 15$  mmHg, and pulmonary vascular resistance  $>3$  Woods unit, meeting the World Health Organization criteria for both 2013 and 2018.<sup>7,8</sup> Furthermore, all patients fulfilled the clinical diagnostic criteria for IPAH, based on objective third-party clinician assessment. Hematoxylin and eosin (H&E) slides of all the lung samples were examined by a pulmonary pathologist for verification of normal lungs and IPAH diagnosis. Clinical information of participants was obtained through electronic medical chart review.

### Processing of lung samples, preparation of single cell libraries, sequencing, and data analysis

Lung samples were brought in Perfadex and processed within 30 min of explant as described previously.<sup>9</sup> Resulting cell suspensions were loaded into 10  $\times$  Genomics Chromium instrument (Pleasanton, CA) for library preparation as described previously.<sup>9</sup> V1 and V2 single cell chemistries were used per manufacturer's protocol. Libraries were sequenced using the Illumina NextSeq-500 platform. Data analysis was performed using R (version 3.2.1). Seurat, an R package developed for single cell analysis, was used for data analysis, normalization of gene expression, and identification and visualization of cell populations.<sup>10</sup> Single Cell Regulatory Network Inference (SCENIC), an R package, was used for identification of transcription factors (TFs) regulating transcriptomes.<sup>11</sup> Cell populations were identified based on gene markers and visualized with t-distributed stochastic neighbor embedding plots. Pathway analysis was performed with Gene Ontology Enrichment Analysis.

## Results

Lung samples were obtained from three patients with IPAH and six normal controls (Table 1). Mean pulmonary arterial pressure of the IPAH patients was 61 mmHg (range 56–69) with mean pulmonary capillary wedge pressure of 14 (range 11–19) on right heart catheterization. Mean pulmonary arterial systolic pressures on transthoracic ECHO of these patients was 117 mmHg (range 86–140) associated with severely decreased right ventricular function in all patients, and moderate (two patients) and severe (one patient) tricuspid regurgitation. All IPAH patients were on a phosphodiesterase-5 inhibitor (tadalafil in two and sildenafil in one patient) and a prostacyclin analog (treprostinil), and two patients were also on an endothelin antagonist (bosentan

**Table 1.** Characteristics of the lung samples included in the study and right heart catheterization hemodynamic parameters of IPAH patients.

ID	Sample status	Age	Gender	# of cells	Chemistry
1	Normal control	76	Male	884	V1
2	Normal control	56	Male	1196/1314	V1
3	Normal control	55	Male	3327	V2
4	Normal control	57	Female	4481	V2
5	Normal control	18	Male	3383	V2
6	Normal control	23	Female	4516/6071	V2
Total		47.5	4 M, 2 F	3146 cells	2 V1, 4 V2
7	IPAH	21	Male	2988	V1
8	IPAH	50	Female	5398	V2
9	IPAH	36	Female	4307	V2
Total		35.6	1 M, 2 F	4231 cells	1 V1, 2 V2
Hemodynamic parameters of IPAH patients					
Mean right atrial pressure ( $\pm$ SD)					12 $\pm$ 4.3
Mean pulmonary arterial pressure ( $\pm$ SD)					61.3 $\pm$ 6.8
Mean pulmonary capillary wedge pressure ( $\pm$ SD)					14 $\pm$ 4.3

IPAH: idiopathic pulmonary arterial hypertension.

or ambrisentan). H&E-stained slides of each lung sample were examined by the pulmonary pathologist confirming the diagnosis of pulmonary arterial hypertension (PAH) (Fig. 1, panels a–c). We examined on an average 3688 cells per sample from nine subjects. The mean age was 47.5 for controls and 35.6 for IPAH. Both controls and IPAH lungs were processed similarly.

Eighteen distinct clusters of cells were identified, and each cluster contained cells from both control and IPAH lungs (Fig. 1, panels d–f). Each cluster was identified based on presence of known markers as described (Table S1).<sup>9,12,13</sup> The EC cluster (cluster #3) was identified by strong, distinctive, and overlapping expression of von Willebrand factor (VWF) and cadherin and platelet EC adhesion molecule (PECAM). The pericytes/smooth muscle (pericyte/SMC) cluster (cluster #13) was identified based on expression of *RGS5* and *DES*. Cells in the pericyte/SMC cluster also expressed previously reported pericyte markers: *CCN1*, *TPM1*, *TPM2*, *CALD1*, and *ACTA2* (Table S1).<sup>12,14</sup> The fibroblast cluster was identified on the basis of *PDGFRA*, *COL1A*, and *COL1A2* expression (cluster #7).<sup>12,13</sup> However, we see very little *POSTN* expression in the fibroblast cluster (cluster 7) in IPAH, indicating that these are not an emergent population as seen in systemic sclerosis associated interstitial lung disease<sup>13</sup> and idiopathic pulmonary fibrosis (IPF, unpublished observations). The monocyte-macrophages and SPP1 macrophage clusters were identified on the basis of expression of *AIF1* and *CD163*, as described.<sup>9</sup> Proliferating cells, identified as described,<sup>9</sup> included macrophages and ECs. The IPAH lung samples did not show a significant difference in number of proliferating ECs compared to control lungs (Fig. 1g).

### Differentially expressed genes and pathway analysis in IPAH vs control pulmonary ECs

We compared gene expression in ECs from IPAH to normal control EC gene expression. Because of the limited number of patients undergoing transplantation for IPAH and thus limited number of IPAH samples, and the large scRNA-seq datasets, we developed three algorithms to parse the data prior to statistical analysis. Namely, we selected the most differentially expressed genes between IPAH and control ECs based on: (1) fold difference of expression between IPAH and control pulmonary ECs; (2) absolute expression level; and (3) specificity of the gene for expression by ECs more highly than all other cell types.

Before selection, there were 33,694 genes in the scRNA-seq dataset. For all three algorithms, we filtered out the genes with fold change <1.5, comparing average IPAH to average control expression, and absolute gene expression <0.3, yielding 1980 genes. We then examined differential gene expression using three different approaches (Fig. S1). In the first approach, we selected only genes with a stringent false discovery rate (FDR) of 10% yielding 33 differentially expressed genes (Table 2). These included genes such as *APLN*, *ENG*, and *KDR* associated with EC growth and angiogenesis, but these genes failed to identify statistically significant pathways on Gene Ontology Enrichment Analysis.

In the second approach (algorithm 2), we used a lenient FDR of 60% to improve the identification of genes that might not be identified otherwise due to type II statistical errors, yet still be important. In the third approach (algorithm 3), we analyzed only genes that were more highly expressed in ECs than any other cell type in our

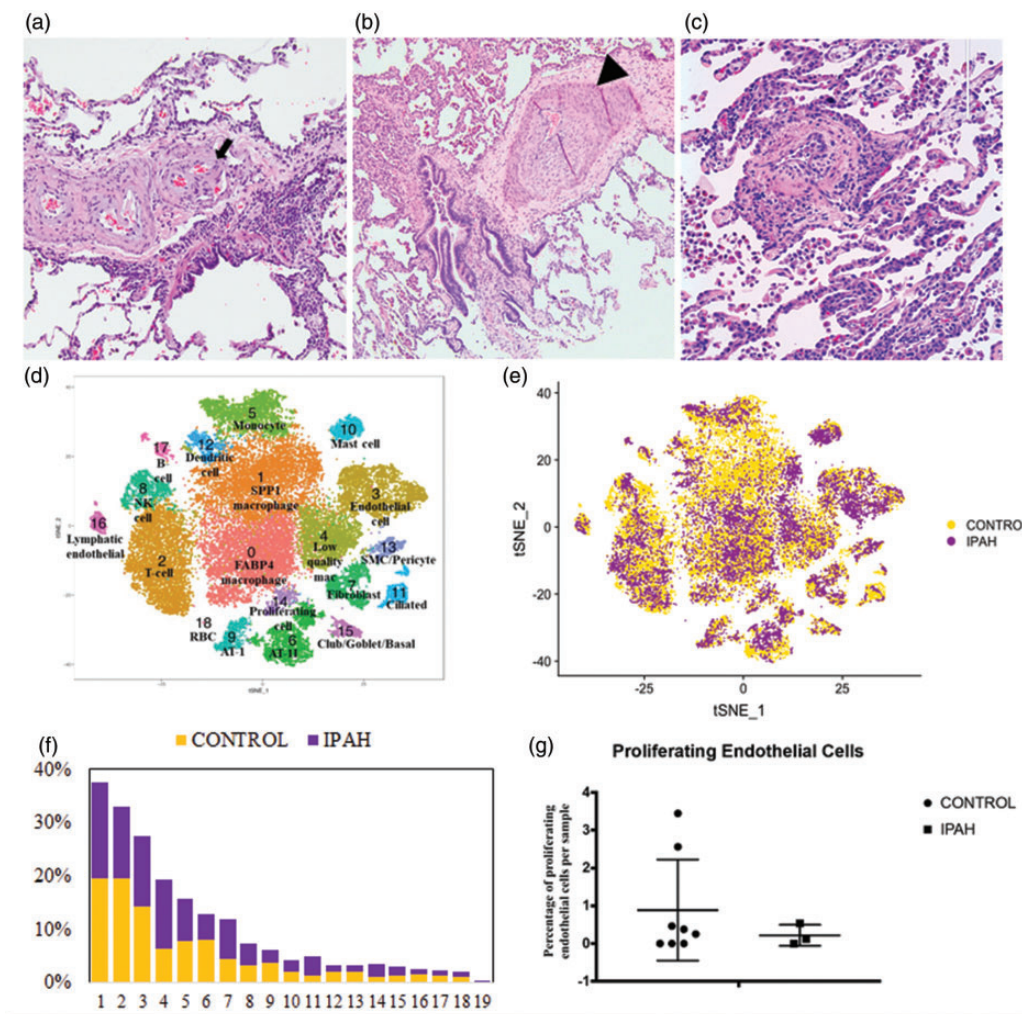


**Fig. 1.** Histopathology of lungs with idiopathic pulmonary arterial hypertension. Histopathology lung explant tissue adjacent to that used for scRNA-seq, showing intimal hyperplasia (arrowhead) and plexiform lesion (arrow) (a–c; magnification 40 $\times$ , 40 $\times$  and 100 $\times$ , respectively), t-SNE plots showing clusters (d) and origin of cells from control (yellow) and IPAH (purple) lungs (e), proportion of control (yellow) and IPAH (purple) cells in each cluster (f), percentage of proliferating endothelial cells in each control and IPAH lungs (g). IPAH: idiopathic pulmonary arterial hypertension.

scRNA-seq dataset to focus the analysis on these genes expressed the highest in ECs. In this approach, we then applied an even less stringent 45% FDR (Fig. S1). With these latter two approaches, 267 and 107 genes were obtained, respectively, for inputting into pathway analyses.

**Gene Ontology Enrichment Analysis.** We used Gene Ontology Enrichment Analysis to identify relationship between differentially regulated genes in IPAH ECs, inputting the gene lists generated by the different algorithms. Despite the lack of any selection for genes most highly expressed by the EC compartment in algorithm 2, both algorithms selected the same top four differentially regulated pathways in IPAH ECs, all associated with cardiovascular/vascular system development: Cardiovascular System Development, Vasculature Development, Blood Vessel Development, and Blood Vessel Morphogenesis (Table 3). Genes upregulated in ECs from IPAH implicated in both blood vessel

development and cardiovascular development included 11 genes: *PRCP*, *RAMP2*, *NOTCH4*, *ROBO4*, *MMRN2*, *HDAC7*, *PDGFB*, *BMP2*, *APLN*, *ENG*, and *END1* (Table 2). There were also unique genes associated with each of these closely related pathways (13 and 11 genes, respectively, for Blood Vessel and Cardiovascular Development pathways).

### Differentially expressed genes and pathway analysis in IPAH vs control pulmonary pericytes

We identified differentially expressed genes between IPAH and control pulmonary pericyte/SMCs, using a similar approach as for ECs, except restricting the analysis to algorithms 1 and 3, because more genes ( $n = 606$ ) were identified using algorithm 2. Selecting genes showing differential expression in IPAH pericytes/SMC compared to control yielded 61 genes using an FDR of 10% (Table 4).

**Table 2.** Top differentially upregulated genes in endothelial cells and Gene Ontology pathways in IPAH.

Endothelial cell genes (10% FDR)		Genes in blood vessel development pathway		Genes in cardiovascular development pathway	
Genes	Fold change	Genes	Fold change	Genes	Fold change
<b>APLN</b>	4.94	<b>PDGFB</b>	6.23	<b>PDGFB</b>	6.23
<i>C1orf54</i>	4.04	<b>APLN</b>	4.94	<b>APLN</b>	4.94
<i>APCDD1</i>	3.61	<b>EDNI</b>	4.10	<b>EDNI</b>	4.10
<i>ORAI2</i>	3.41	<i>COL4A2</i>	3.67	<u><i>SOX18</i></u>	4.07
<i>ENG</i>	3.29	<i>LAMA4</i>	3.46	<b>ENG</b>	3.29
<i>COL6A3</i>	3.15	<b>ENG</b>	3.29	<i>COL4A1</i>	3.06
<i>LAGE3</i>	2.65	<i>AMOTL2</i>	2.89	<b>NOTCH4</b>	2.87
<i>RSBN1L</i>	2.41	<b>NOTCH4</b>	2.87	<i>SMAD6</i>	2.79
<i>KLF16</i>	2.39	<u><i>HDAC7</i></u>	2.62	<u><i>HDAC7</i></u>	2.62
<i>KNOP1</i>	2.38	<i>NDST1</i>	2.34	<i>ARHGEF15</i>	2.11
<i>GAS6</i>	2.27	<i>TNFSF12</i>	2.21	<i>PLXND1</i>	2.09
<i>LARPI</i>	2.22	<b>PRCP</b>	2.00	<i>ESM1</i>	2.06
<u><i>FAM60A</i></u>	2.21	<i>KDR</i>	1.95	<b>PRCP</b>	2.00
<i>PNPLA4</i>	2.21	<b>ROBO4</b>	1.91	<b>ROBO4</b>	1.91
<i>DIMT1</i>	2.20	<b>MMRN2</b>	1.83	<i>HEG1</i>	1.88
<i>GK5</i>	2.18	<b>RAMP2</b>	1.79	<i>ROM1</i>	1.88
<i>LDOC1</i>	2.14	<i>FGFR1</i>	1.79	<b>MMRN2</b>	1.83
<u><i>TFDPI</i></u>	2.10	<u><i>LYL1</i></u>	1.76	<b>RAMP2</b>	1.79
<u><i>STRA13</i></u>	2.01	<u><i>ELK3</i></u>	1.76	<i>ADAM15</i>	1.74
<i>UTP4</i>	1.98	<b>ARID1A</b>	1.75	<i>NOTCH1</i>	1.53
<i>TAOK2</i>	1.96	<i>PRKACA</i>	1.55	<b>BMPR2</b>	1.52
<i>KDR</i>	1.95	<b>BMPR2</b>	1.52	<i>RASIP1</i>	1.51
<i>PRRC2A</i>	1.87	<i>MYO1C</i>	1.51		
<i>DOCK6</i>	1.84	<i>SEC24B</i>	1.50		
<i>REV1</i>	1.83				
<i>FAM89A</i>	1.83				
<i>SLC10A3</i>	1.82				
<i>WDR77</i>	1.76				
<i>IGFBP4</i>	1.75				
<b>ARID1A</b>	1.75				
<i>SH3KBP1</i>	1.71				
<i>VOPPI</i>	1.51				
<i>ARL6IP4</i>	1.50				

FDR: false discovery rate.

Note: Bolded genes are common in multiple pathways and underlined genes are transcription factors and epigenetic modifiers.

Gene Ontology Enrichment Analysis did not yield any significant pathways.

Filtering 33,694 genes with fold change >1.5, absolute gene expression >0.3, and selecting only genes that were expressed most highly in pericyte/SMCs with 45% FDR yielded 206 genes (Fig. S1, algorithm 3). Inputting these genes into Gene Ontology Enrichment Analysis yielded top differentially regulated pathways, including Negative Regulation of Cell Development, Developmental Processes and Cell Differentiation, Anatomical Structure Morphogenesis, Extracellular Matrix Organization,

Extracellular Structure Organization, and Circulatory System Development (Table S2); 29 genes were found to be in Circulatory System Pathway (Table 4). Many of the genes in this pathway overlapped with those seen in the other pathways (Table 4, bolded genes).

#### *Differentially expressed genes and pathway analysis in IPAH vs control pulmonary fibroblasts*

We identified differentially expressed genes in IPAH compared to control lung fibroblasts, since adventitial

**Table 3.** Top upregulated Gene Ontology pathways in endothelial cells in IPAH.

	No. of genes	Fold-change	FDR
Endothelial cell pathways (Algorithm 2)			
Blood vessel development	24	3.9	4.89E-04
Cardiovascular system development	24	3.65	5.26E-04
Vasculature development	24	3.72	5.59E-04
Blood vessel morphogenesis	19	3.71	7.02E-03
Tube morphogenesis	23	2.81	3.97E-02
Angiogenesis	15	3.76	5.09E-02
Tube development	26	2.45	1.11E-01
Circulatory system development	26	2.41	1.14E-01
Renal system process	8	5.79	1.80E-01
Positive regulation of epithelial cell migration	9	5.11	1.86E-01
Regulation of epithelial cell migration	11	4.06	1.90E-01
RNA processing	25	2.28	1.91E-01
Extracellular structure organization	15	3.11	1.99E-01
Regulation of endothelial cell migration	9	4.64	2.21E-01
Regulation of blood vessel endothelial cell migration	7	6.21	2.31E-01
Positive regulation of endothelial cell proliferation	7	6.01	2.45E-01
Regulation of endothelial cell proliferation	8	5.05	2.56E-01
Negative regulation of glial cell apoptotic process	3	29.6	2.61E-01
Positive regulation of endothelial cell migration	7	5.7	2.79E-01
Regulation of glial cell apoptotic process	3	26.31	2.95E-01
tRNA processing	8	4.78	3.08E-01
Extracellular matrix organization	13	3.06	3.39E-01
ncRNA processing	14	2.88	3.61E-01
Anatomical structure morphogenesis	45	1.69	4.05E-01
Regulation of cell motility	24	2.13	4.06E-01
Regulation of cell migration	23	2.2	4.12E-01
Cellular process	208	1.14	4.87E-01
RNA metabolic process	37	1.76	4.95E-01
Positive regulation of blood vessel endothelial cell migration	5	7.18	5.02E-01
Endothelial cell pathways (Algorithm 3)			
Cardiovascular system development	22	8.64	1.13E-10
Vasculature development	22	8.81	1.55E-10
Blood vessel development	20	8.39	2.35E-09
Blood vessel morphogenesis	18	9.08	8.37E-09
Circulatory system development	24	5.74	1.26E-08
Anatomical structure morphogenesis	36	3.49	2.56E-08
Angiogenesis	15	9.71	1.39E-07
Tube morphogenesis	20	6.32	1.42E-07
Tube development	22	5.36	2.33E-07
Anatomical structure formation involved in morphogenesis	22	5.1	5.18E-07
Regulation of cell motility	21	4.82	3.13E-06
System development	49	2.29	3.26E-06
Regulation of cell migration	20	4.93	5.09E-06
Regulation of locomotion	21	4.45	1.08E-05
Regulation of cellular component movement	21	4.42	1.12E-05
Developmental process	55	1.97	1.92E-05
Anatomical structure development	53	2.02	1.98E-05
Multicellular organism development	50	2.05	3.54E-05
Cellular developmental process	42	2.29	3.87E-05

FDR: false discovery rate.

**Table 4.** Top differentially upregulated genes in pericyte/SMCs (10% FDR) and in select Gene Ontology pathways in IPAH.

10% FDR				Circulatory system development		Negative regulation of cell development, differentiation, and developmental process <sup>a</sup>		Extracellular matrix and structure organization <sup>b</sup>	
Genes	Fold change	Genes	Fold change	Genes	Fold change	Genes	Fold change	Genes	Fold change
ABCA8	5.44	<b>MFAP2</b>	6.06	<b>ABLI</b>	1.54	<b>ABLI</b>	1.54	<i>CCDC80</i>	4.05
ADGRF5	2.28	<i>MRPL23</i>	2.2	<b>COL18A1</b>	3.77	<i>ACTN4</i>	2.39	<i>COL14A1</i>	1.76
AFAP1	3.35	<i>NEURL1B</i>	2.45	<b>COL5A1</b>	4.82	<i>CHRD</i>	3.4	<b>COL18A1</b>	3.77
ANXA6	1.84	<i>NFATC3</i>	2.6	<b>ECM1</b>	3.17	<b>COL5A1</b>	4.82	<b>COL5A1</b>	4.82
AP3S1	1.92	<i>NME3</i>	1.59	<i>EDNRA</i>	2.02	<b>COL5A2</b>	2.05	<b>COL5A2</b>	2.05
BCL2L1	1.54	<i>NPDC1</i>	2.64	<i>ELN</i>	1.65	<b>ECM1</b>	3.17	<i>EGFL6</i>	2.3
<i>CI1orf74</i>	3.37	<i>NSMCE4A</i>	2.31	<i>FBXW7</i>	3.43	<i>FBXW7</i>	3.43	<b>ELN</b>	1.65
<i>CAND1</i>	2.07	<i>ORAI2</i>	4.02	<i>FHL2</i>	1.64	<i>FKBP4</i>	1.65	<i>ITGA1</i>	1.94
<i>CBWD2</i>	3.27	<b>PBX1</b>	6.93	<i>JAG1</i>	5.31	<i>FRZB</i>	3.83	<i>ITGA8</i>	3.19
<i>CDC5L</i>	2.7	<i>PFDN6</i>	3.63	<i>LTBP1</i>	1.77	<i>GDF10</i>	1.53	<i>ITGB5</i>	1.82
<i>CHTF8</i>	1.62	<i>PGM5</i>	2.42	<i>MCAM</i>	1.57	<i>GDI1</i>	1.96	<i>MFAP2</i>	6.06
<b>COL18A1</b>	3.77	<i>PHF14</i>	3.77	<i>MED1</i>	7.02	<i>HOOK3</i>	1.51	<i>MFAP4</i>	3.2
<i>CREBZF</i>	2.83	<i>PQLC1</i>	6.9	<i>MEIS1</i>	6.64	<i>ITM2C</i>	2.68	<b>MYH11</b>	1.9
<i>CUL5</i>	3.18	<i>PQLC3</i>	2.81	<b>MYH11</b>	1.9	<i>JAG1</i>	5.31	<b>NFI</b>	3.38
<i>DCTPP1</i>	3.39	<i>PTPRA</i>	2.76	<b>NFI</b>	3.38	<b>LPAR1</b>	8.14	<i>NPNT</i>	1.77
<i>DEXI</i>	4.81	<i>RBM14</i>	2.71	<i>NTRK2</i>	1.7	<i>MED1</i>	7.02	<i>OLFML2B</i>	1.86
<i>DTX3</i>	1.86	<i>RERG</i>	3.08	<i>NTR3</i>	1.74	<i>MEIS1</i>	6.64	<i>PLTP</i>	3.3
<i>EFEMP1</i>	2.99	<i>RFC2</i>	2.54	<i>PCSK5</i>	6.71	<b>NFI</b>	3.38	<b>PTK2</b>	3.52
<i>FLII</i>	3.85	<i>RFK</i>	2.34	<i>PDGFRB</i>	1.76	<i>NTRK3</i>	1.74	<b>SPARC</b>	1.59
<i>FUNDC1</i>	2.02	<i>RPL26L1</i>	2.2	<i>PGF</i>	2.44	<i>PBX1</i>	6.93		
<i>GTPBP6</i>	1.93	<i>RSRC1</i>	3.54	<i>PLXDC1</i>	3.06	<b>PTK2</b>	3.52		
<i>HGSNAT</i>	5.2	<i>SAFB2</i>	2.29	<b>PTK2</b>	3.52	<i>RUNXIT1</i>	2.89		
<i>HOTAIRM</i>	1.59	<i>SDHAF1</i>	2.37	<i>SLIT3</i>	2.26	<b>SMAD4</b>	3.01		
<b>ITGA1</b>	1.94	<i>SLC30A5</i>	1.94	<b>SMAD4</b>	3.01	<i>SNAPIN</i>	8.99		
<i>KAT5</i>	1.65	<i>SLC41A3</i>	2.97	<i>SMARCD3</i>	5.41	<b>SPARC</b>	1.59		
<i>KLHDC10</i>	2.97	<i>SMC6</i>	2.37	<b>SPARC</b>	1.59	<i>STARD13</i>	5.89		
<b>LPAR1</b>	8.14	<i>SNAPC3</i>	1.9	<b>TBX2</b>	1.62	<b>TBX2</b>	1.62		
<i>LTBP3</i>	2.21	<i>SNX21</i>	5.12	<b>THY1</b>	7.72	<b>THY1</b>	7.72		
<i>MAGED1</i>	4.62	<i>TCF7L2</i>	2.31	<b>ZFP36L1</b>	1.66	<b>ZFP36L1</b>	1.66		
<i>METRNL</i>	6.07	<i>TMEM67</i>	16.72						
		<i>WRB</i>	2.53						

<sup>a</sup>*ABLI*, *ECM1*, *SPARC*, *STARD13*, and *TBX2* were found only in negative regulation of developmental process pathway.

<sup>b</sup>*PLTP* gene was found only in extracellular structure organization pathway.

Note: Bolded genes are common in multiple pathways.

FDR: false discovery rate.

fibroblasts have been implicated in PAH pathogenesis.<sup>15</sup> Using the same approach as that for analyzing pericyte/SMCs, genes were identified showing higher expression in IPAH compared to control fibroblasts, using an FDR of 10%, and genes most highly expressed by fibroblasts comparing IPAH with control fibroblasts using an FDR of 45% (Fig. S1, Table S3), the former not yielding significant pathways on Gene Ontology Enrichment. Gene Ontology

Enrichment Analysis inputting upregulated fibroblast genes at FDR of 45% identified several pathways, including Gene Matrix Organization, as well as Regulation of WNT and Response to TGF $\beta$  (Table S4A). Ten genes were associated with the extracellular matrix pathway and three and five genes associated with the Regulation of WNT Signaling and Response to TGF $\beta$  Signaling pathways, respectively (Table S4B).

### Differentially expressed genes and pathway analysis in IPAH vs control pulmonary monocyte-macrophages and SPP1 macrophages

We sought to identify differentially expressed genes between IPAH and control pulmonary monocyte-macrophage, and SPP1 macrophages based on our previous observations of these macrophage subpopulations,<sup>9</sup> using a similar approach to above. Filtering 33,694 genes with fold change >1.5, absolute gene expression >0.3, and selecting genes that were differentially expressed at a 10% FDR threshold most highly in monocyte-macrophages yielded 16 genes and for SPP1 macrophages, 18 genes (Table S5). Selecting genes more highly expressed in each of the SPP1 and monocyte-macrophage subsets compared to other cell cluster yielded only 134 and 17 genes, respectively, even without an FDR selection. As none of these selection criteria yielded statistically significant pathways on Gene Ontology analysis, we did not pursue further analyses.

### Predicted TFs in regulating IPAH transcriptome

In order to identify TFs that might play important roles in the dysregulated IPAH EC phenotype, we analyzed the EC

transcriptome data using SCENIC, a computational method for gene regulatory network reconstruction from scRNA-seq datasets.<sup>11</sup> SCENIC implicated 39 TFs as regulating IPAH EC transcriptome (Fig. 2a). However, of the TFs upregulated in IPAH ECs analyzed by SCENIC, including *SOX18*, *STRA13*, *LYLI*, *ELK*, and *TFDPI*, only *SOX18* showed a pattern of regulon expression that overlaid strongly with IPAH ECs (Fig. 2b). This mirrored the level of expression of *SOX18* in IPAH cells (Fig. 2c and d).

### Genes associated with hereditary PAH are selectively expressed in ECs, pericytes/SMC, and dendritic cells

To clarify the cell types expressing genes that have been shown mutated in hereditary PAH, we examined their expression in our scRNA-seq data. This analysis supported the highly selective, though not exclusive, expression of *BMPR2*, *ACVRL1*, and *ENG* on ECs, with modestly increased expression of *BMPR2* (1.52-fold), no change in *ACVRL1* (1.0-fold), and upregulated expression of *ENG* (3.29-fold) by PAH compared to control ECs (Fig. 3). These three genes were also expressed at lower levels by macrophages. *SMAD9* and *SOX17* were expressed almost exclusively by ECs, and *SMAD9*, but not *SOX17*,

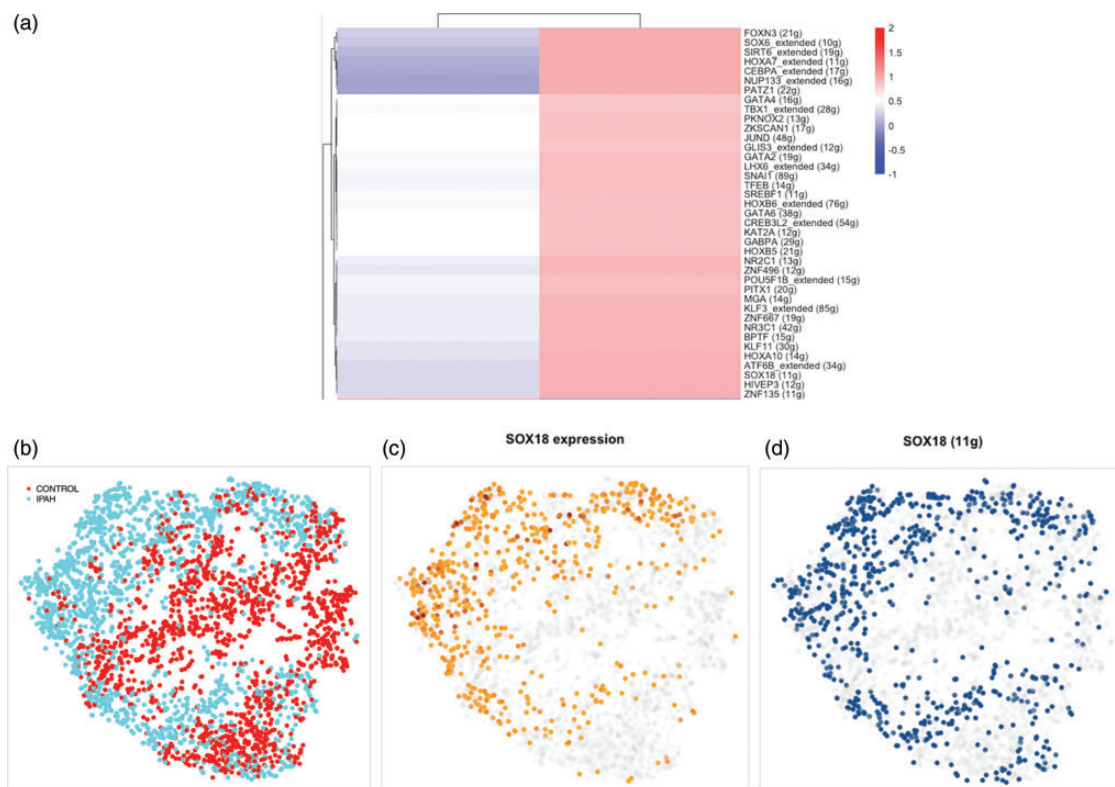


**Fig. 2.** Regulon and predicted transcription factors regulating endothelial cell transcriptome expression in IPAH endothelial cells. Cluster of transcription factors predicted to be upregulated in IPAH endothelial cells (panel a). T-SNE clustering by regulon (panels b–d), showing the origin of the cells: IPAH (blue) versus control (red) lung explants (panel b). *SOX18* expression in regulon t-SNE is indicated by intensity of yellow/brown color (panel c). Level of *SOX18* regulon activity in *SOX18* regulon t-SNE is indicated by intensity of blue color (panel d). IPAH: idiopathic pulmonary arterial hypertension.

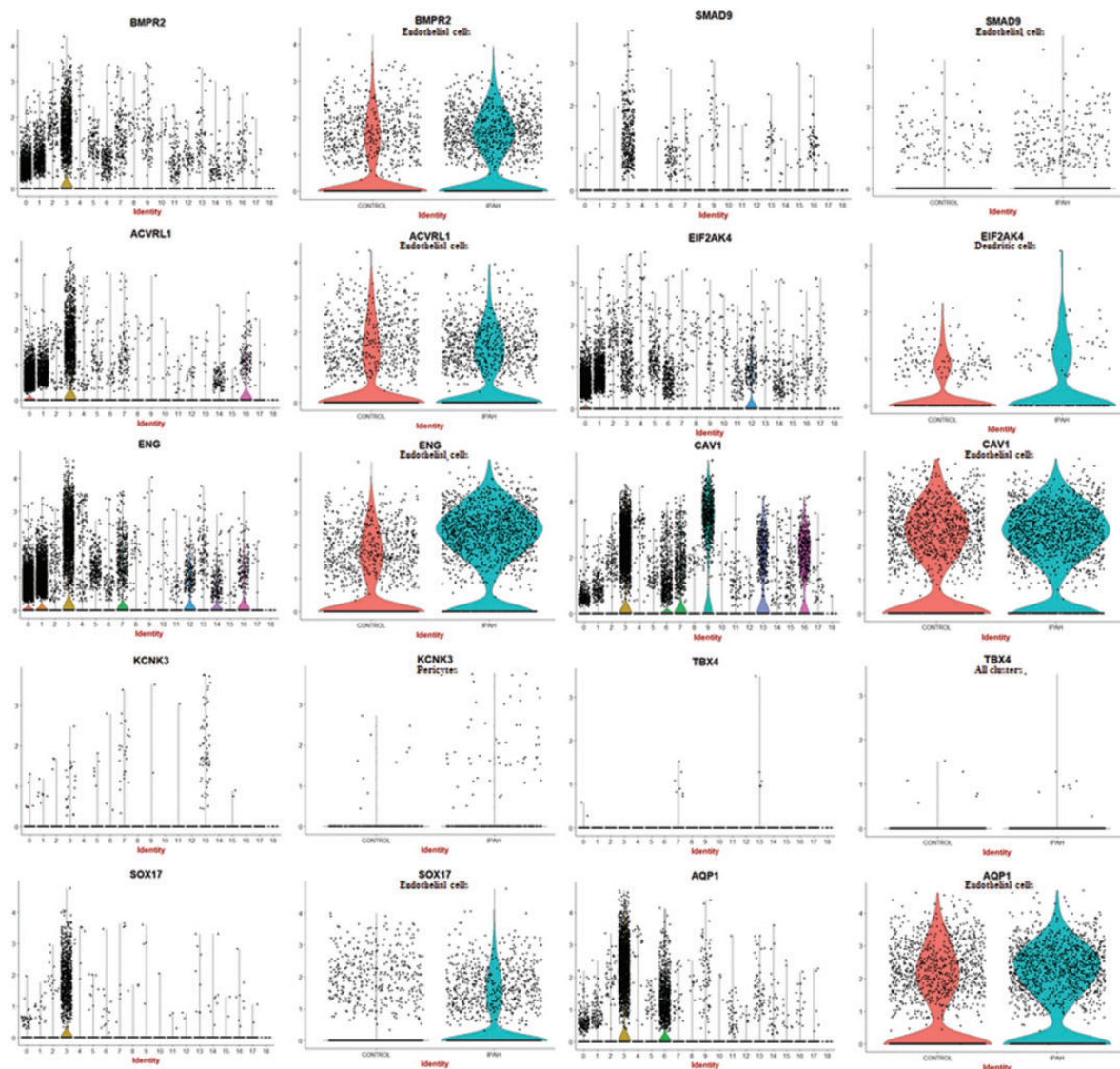


**Fig. 3.** Expression of genes associated with hereditary IPAH in different cell types. Violin plots indicate expression of genes associated with hereditary IPAH in each cluster (cluster numbers as in Fig. 1) of cells from both IPAH and control lungs (panels on left). Violin plots showing expression of the cell type with the highest expression in left panels, show expression divided between control and IPAH lungs (panels on the right). For most genes, highest expression is cluster #3 (endothelial cells). For *KCNK3*, highest expression is in pericytes (cluster #13). For *EIF2AK4* highest expression is in dendritic cells (cluster #12).

upregulated on IPAH ECs (*SMAD9*: 1.99-fold; *SOX17*: 1.05-fold). *AQP1* was also expressed selectively on ECs, but also by alveolar type II cells, showing relatively little difference in expression comparing IPAH to control ECs (1.20-fold). In contrast, *KCNK3* was most highly expressed by pericytes and highly upregulated in IPAH compared to control ECs (8.18-fold). *EIF2AK4* was expressed by many cell types, including macrophages and dendritic cells. *CAV1* was expressed highly by ECs but more highly by type I alveolar cells, as well as pericyte/SMCs and lymphatic ECs. *TBX4* was detected only at very low levels in fibroblasts and pericyte/SMCs. Thus, of the genes associated with hereditary PAH, *ENG* and *SMAD9* were the most

upregulated in IPAH ECs and *KCNK3* in pericytes, with the other genes showing no or modest regulation.

#### *ScRNA-seq data are validated by and extend bulk microarray data*

The recent analysis of a large database of microarray data from IPAH and control lungs provided a robust opportunity to confirm regulation of genes found in our dataset.<sup>16</sup> Our scRNA-seq data in turn provided the opportunity to significantly extend bulk lung gene expression observations by showing which cells are expressing genes shown to be regulated in bulk lung expression data. To show the utility

in this approach, we compared bulk microarray RNA expression by IPAH ( $n=31$ ) and failed donor lungs ( $n=25$ , NCBI GEO, GSE117261<sup>16</sup>) with our scRNA-seq data, selecting the 10 most statistically significant upregulated genes in bulk microarray for comparison (Table S6). Two of the most statistically significant upregulated genes were Hemoglobin genes (hemoglobin subunit beta and hemoglobin subunit alpha 2//hemoglobin subunit alpha 1), which were both expressed most highly in scRNA-seq erythrocyte cluster #18 (not shown), and one of the genes, *GGTAIP*, was not seen in the scRNA-seq data. Six of the seven other genes showed increased expression in specific cells types: *FZD7* in IPAH pericyte/SMCs, *ECM2*, and *RARRES2* in IPAH fibroblasts, *LTBP1* and *PDE3A* in IPAH fibroblasts and pericyte/SMCs, and *PDE7B* in IPAH ECs, fibroblasts, pericyte/SMCs, and mast cells (Fig. S2). We include a full dataset of gene expression in each cluster, each sample, and each gene (Table S7A) in addition to average expression of each gene in IPAH and control lungs for each gene (Table S7B) providing reference databases for investigators (see <http://dom.pitt.edu/rheum/centers-institutes/scleroderma/systemicscleroticcenter/database/>).

## Discussion

Comparing transcriptomic profiles of different cell types in healthy and IPAH lungs by scRNA-seq, we found that ECs and pericyte/SMCs displayed the most differentially expressed genes between IPAH and normal lungs compared to other cell types. As such, our results reinforce the important role of ECs and pericyte/SMCs in IPAH pathogenesis. Among the EC genes that were most differentially upregulated in IPAH: *ENG*, *Orai2*, *TFDP1*, *KDR*, *AMOTL2*, *PDGFB*, *FGFR1*, *EDN1*, and *NOTCH1* have been previously reported in the literature and support the broader validity of our results.<sup>17-23</sup> The Pulmonary Hypertension Breakthrough Initiative has provided the largest transcriptome study data to date.<sup>16</sup> Our data complement this study, representing the first close look at the transcriptomic landscape across IPAH lung cells in vivo, thus allowing for cell-specific analysis not possible with prior findings in cultured cells or whole lung transcriptomic analysis.

Our data show several cytokine and cytokine receptor genes upregulated in IPAH ECs, likely contributing in an autocrine fashion to the altered phenotype of ECs as well as in a paracrine fashion to pericyte/SMC hyperplasia in IPAH. This includes upregulated EC expression of platelet derived growth factor-beta (PDGF- $\beta$ ), endothelin-1, and Apelin (*APLN*), and of the receptors VEGFR-2 (*KDR*), *BMPR2*, *ENG*, and *FGFR1*. As such, EC expression in IPAH appears to strongly support roles for multiple growth factors that regulate angiogenesis, robustly supported also by the pathway analyses.

*FGFR1* has been shown upregulated in pulmonary arterial ECs<sup>24</sup> associated with decreased *APLN* expression. In

recently reported bulk data,<sup>16</sup> *FGFR1* showed 1.19-fold and *APLN* showed 1.56-fold increased expression. Our data showed both of these genes increased in IPAH ECs. *APLN*, a peptide that binds to apelin receptor (*APLNR*),<sup>25</sup> promotes angiogenesis through activation of extracellular-signal-regulated kinases, Akt, and p70S6kinase, and has vasodilator properties through induction of nitric oxide release.<sup>26</sup> Previous studies showed reduced *APLN* mRNA levels and *APLN* expression in cultured ECs from IPAH compared to control lungs.<sup>24</sup> Furthermore, administration of *APLN* was shown to reverse PAH in mice. Our study challenges these data on the role of *APLN* in IPAH, indicating that not only *APLN* but also the Apelin cleaving enzyme Lysosomal Pro-X carboxypeptidase (*PRCP*),<sup>27</sup> a protein also described to promote angiogenesis and vascular repair,<sup>28</sup> show elevated expression by PAH ECs.

IPAH ECs also showed upregulated expression of endoglin (*ENG*, 3.29-fold), encoding a Transforming growth factor-beta (TGF $\beta$ ) signaling co-receptor that is highly expressed on ECs and controls EC differentiation, proliferation, and angiogenesis. Loss of function *ENG* mutations leads to hereditary hemorrhagic telangiectasia (HHT) type 1, an autosomal dominant syndrome characterized by vascular dysplasia associated with PAH.<sup>29</sup> Relatively frequent mutations in the *ENG* gene associated with PAH have been described, although the role of these in disease is uncertain.<sup>18</sup> However, in PAH, *ENG* expression has been reported as elevated on IPAH ECs, consistent with our scRNA-seq observation.<sup>30</sup> In distinction from HHT patients in whom deficient *ENG* is associated with PAH, in mice *ENG* deficiency is protective for hypoxic pulmonary hypertension. The apparent paradox between the development of PAH in both settings of deficient and upregulated gene expression has been considered in regard to Fibroblast growth factor (FGF).<sup>31</sup> A similar paradox is presented by our data, which show increased *ENG*, in PAH, even though genetic data indicate that deficient function of these receptors is associated with PAH. In addition to elevated *ENG* expression, PAH ECs also showed modestly increased expression of *BMPR2* (1.52-fold), the most common gene mutated in familial PAH and associated with deficient function. In comparison, bulk lung IPAH mRNA *BMPR2* expression showed no change (1.00-fold) compared to control lungs (from NCBI GEO, GSE117261<sup>16</sup>). These results suggest an uncoupling between *BMPR2* mRNA and protein expression, as *BMPR2* protein expression has been shown previously to be downregulated in IPAH by immunohistochemistry.<sup>32</sup>

In addition to the several cytokines and cytokine receptors already implicated in IPAH, we saw upregulated expression of several other genes involved in regulating EC growth: *ROBO4*, an endothelial receptor that regulates endothelial migration<sup>33</sup> and stabilizes the endothelium by opposing signaling by *VEGF*;<sup>34</sup> *APCDD1*, an inhibitor of Wnt signaling pathway in which overexpression is associated with increased paracellular barrier permeability by

retinal endothelium and shown to coordinate the timing of vascular pruning and barrier maturation;<sup>35</sup> *NDST1*, a bifunctional enzyme that catalyzes both the N-deacetylation and the N-sulfation of glucosamine of the glycosaminoglycan in heparan sulfate, which regulates BMP signaling and internalization in lung development by affecting the binding of BMP to extracellular matrix;<sup>36</sup> and *MMRN2*: (Multimerin2), also known as Endoglyx-1, an extracellular matrix glycoprotein that binds to and inhibits the activity of VEGFA.<sup>37,38</sup>

Two genes implicated directly (*NOTCH4*) or indirectly (*DOCK6*) in the NOTCH pathway were upregulated. *NOTCH4* is expressed exclusively in ECs as opposed to other NOTCH subtypes. Constitutively active endothelial *NOTCH4* inhibits EC apoptosis,<sup>39</sup> and is associated with brain and lung arteriovenous malformations in mice,<sup>40</sup> suggesting roles of *NOTCH4* in EC survival and vascular integrity. *DOCK6* is a guanine nucleotide exchange factor regulator of Cdc42 that activates Rho family guanosine triphosphatases, Rac1 and Cdc42, and is required for normal function of the actin cytoskeletal structure. Autosomal recessive forms of Adams–Oliver syndrome can be due to mutations in *EOGT*, which encodes a component of Notch pathway, or *DOCK6* mutations.<sup>41–43</sup> Autosomal dominant forms are caused by mutations in *NOTCH1*, *RBPJ*, or *DLL4* (all NOTCH pathway components) or *ARHGAP31*, which encodes another Rho GTPase regulator. Patients with Adams–Oliver syndrome who have *DOCK6* mutations develop dilated surface blood vessels, pulmonary or portal hypertension, and retinal hypervascularization.

Several TFs upregulated in IPAH ECs, including *SOX18*, *STRA13*, *LYL1*, and *ELK*, have known roles in regulating EC phenotype. *SOX18*, expressed four times higher in IPAH than control ECs, regulates vasculature development and endothelial barrier integrity.<sup>44–46</sup> In an ovine model of congenital heart disease with shunt, *SOX18* expression was upregulated in pulmonary arterial ECs, correlating with increased trans-endothelial resistance.<sup>47</sup> Thus, upregulation of *SOX18* in IPAH might be a primary alteration driving EC microangiopathy and obliterative changes, or an adaptive change to high shear stress. Notably, of all the TFs analyzed by SCENIC, it showed the most robust regulon and associated increased expression in IPAH ECs, suggesting that it plays a critical role in the altered IPAH transcriptome. *STRA13* is a basic helix-loop-helix (bHLH) TF that is upregulated during hypoxia by HIF1 $\alpha$ /VHL. It plays important roles in the regulation of cell proliferation, differentiation, and apoptosis.<sup>48</sup> Both Stat1 and Stat3 are targets of *STRA13*, *STRA13* mediating hypoxic repression of Stat1,<sup>49</sup> *STRA13* also binding to Stat3.<sup>50</sup> *LYL1* is a bHLH TF and a major regulator of adult neovascularization.<sup>51</sup> *LYL1* and *TAL1*, another bHLH TF, along with a cofactor LIM-only-2 protein regulate EC transcription of Angiopoietin-2 a major regulator of angiogenesis.<sup>52</sup> *ELK3* is a transcriptional repressor that is downregulated during hypoxia, releasing repression of several genes and leading to

increased expression of Egr1 and VEGF, as well as PHD2, PHD3, and Siah2 destabilizing HIF1 $\alpha$ .<sup>53–55</sup> Thus, its elevated expression is surprising and might be expected to inhibit angiogenesis. *TFDP1*, a TF that regulates proliferation, apoptosis, and differentiation of myeloid cells was also upregulated in ECs.<sup>56–59</sup> *TFDP1* complexes with E2F and regulates a series of genes involved in cell cycle, suggesting that its elevation in IPAH might promote EC proliferation.<sup>60</sup> Most likely, these TFs work in combination to alter the transcriptome and phenotype of IPAH ECs.

In addition to insights in TFs regulated in IPAH, upregulated expression of *FAM60A* and *HDAC7* indicate important epigenetic changes are occurring in IPAH ECs. *FAM60A/SINHCAF* is part of the SIN3A–HDAC complex, a master transcriptional repressor that is required for a complete response to hypoxia.<sup>61</sup> *FAM60A/SINHCAF* specifically represses HIF2 $\alpha$  mRNA and protein expression by interacting with the TF SP1 and recruitment of HDAC1 to the HIF2 $\alpha$  promoter.<sup>62</sup> *HDAC7* is a class IIa histone deacetylase with a well described role in regulating angiogenesis. Mice deleted of *HDAC7* show loss of endothelial cell–cell adhesion, vascular dilation, and rupture.<sup>63</sup> *HDAC7* is also required in vitro for EC migration and tube formation.<sup>64</sup> *HDAC7* epigenetically regulates *MMP10* and *AKAP12*, a suppressor of angiogenesis.<sup>65</sup> VEGFA stimulates *HDAC7* phosphorylation and shuttling into the nucleus.<sup>66</sup>

Examining genes showing increased expression by pericyte/SMCs, meeting the 10% FDR revealed several genes implicated in regulating cellular apoptosis: *BCL2L1*,<sup>67</sup> *FUNDC1*,<sup>68</sup> and *KLHDC10*;<sup>69</sup> Lysophosphatidic acid signaling: *LPAR1*;<sup>70</sup> and muscle and smooth muscle cell differentiation and growth: *MAGED1*<sup>71</sup> and *NFATC3*.<sup>72</sup> Several TFs and epigenetic regulators were upregulated in IPAH pericyte/SMCs. *PBX1* encodes a TF that works cooperatively with *KLF4* and *MEIS2*;<sup>73</sup> cooperates with *MYOD1* in myoblast differentiation;<sup>74</sup> is expressed widely in developing mesenchymal tissues including smooth muscle; and its deletion leads to pulmonary hypertension associated with elevated *MYH11* and *EDN1* in whole lungs.<sup>75</sup> *PHF14*, suggested to be an epigenetic regulator through binding to histones, has been implicated in lung development and its deletion in a neonatal case of pulmonary hypertension.<sup>76,77</sup> *SAFB2* encodes a transcriptional repressor<sup>78</sup> and *TCF7L2*, a TF involved in Wnt signaling, mutated in diabetes mellitus type 2, and important in pancreatic pericyte function.<sup>79</sup>

Examining genes in IPAH pericytes ECM pathway analysis showed upregulated expression of multiple ECM proteins and integrins, suggesting that these cells have converted to a profibrotic phenotype characterized in particular by increased expression of *COL14A1*, *COL18A1*, *COL5A1*, *COL5A2*, *ELN*, *ITGA1*, *ITGA8*, *ITGB5*, *MFAP2*, *MFAP4*, *OLFML2B*, and *SPARC*. Notably, *COL18A1* is cleaved to form endostatin, an inhibitor of angiogenesis.<sup>80</sup>

IPAH pericytes also expressed several ligands for genes showing increased expression in IPAH ECs. *SLIT3* was upregulated on IPAH pericyte/SMCs while its cognate ligand *ROBO4* was upregulated on IPAH EC;<sup>81</sup> *PDGFRB* was upregulated in IPAH pericyte/SMCs while its growth factor ligand *PDGFB* was upregulated in IPAH ECs; and *JAG1* was upregulated on IPAH pericyte/SMCs while its cognate ligand *NOTCH1* was upregulated on IPAH ECs. Thus, it appears IPAH pericyte/SMCs might be acting to facilitate or alter the IPAH EC phenotype through several of these interacting receptor–ligand pairs. Finally, both *ITGA8* and its cognate ligand *NPNT*, associated with arrector pili muscle development in skin,<sup>82</sup> were upregulated on IPAH pericyte/SMCs, suggesting possible autocrine role in pericyte hypertrophy.

Monocyte-derived macrophages have been implicated in PAH in several studies in hypoxia-induced disease,<sup>83–86</sup> and these cells implicated as potential mesenchymal progenitors.<sup>85</sup> We did not see evidence for monocyte-macrophage co-expression of *COL1A1* to suggest a population of monocyte-macrophage mesenchymal progenitors. Changes in gene expression in macrophage populations in IPAH lungs were modest and relatively few differentially expressed genes met a 10% FDR, compared to EC and pericyte/SMC regulated genes, suggesting that in late stage IPAH, macrophage populations may not be as active or may display more heterogeneous or individualized roles not discernible through this analysis.

There are several limitations to this study. Most important is the relatively small sample size. As IPAH patients come to transplant relatively infrequently, this is an inherent limitation related to their clinical course. To mitigate this limitation, we placed other limitations on the data, examining only upregulated genes, and for pathway analysis allowing liberal FDRs, which leads to a lack of conclusive statistical rigor for some of the genes associated with the pathway analyses. This is partially mitigated by the highly statistically significant pathway associations of these genes. However, the most reliable alterations in gene expression are represented by our initial analysis using a 10% FDR. The other major limitation is that lung explants represent end-stage disease in patients who are heavily treated with vasodilators. It is possible that some of the changes in gene expression identified in this study are representative of only late-stage disease and/or are changes that are reactive to therapies. For example, it is known that treatment with endothelin antagonists is associated with increased plasma levels of endothelin-1.<sup>87</sup> As IPAH patients almost never undergo lung biopsies, these limitations cannot be overcome under current standard of care. Despite these limitations, this approach analyzes the cells under conditions in which there is ongoing pulmonary hypertension and assesses gene expression within hours of lung explant. As such, it provides a robust, transcriptomic landscape of IPAH lungs, showing major changes in gene expression

of ECs, pericyte/SMCs, and fibroblasts in IPAH pathology, implicating multiple novel genes in IPAH pathogenesis.

### Contribution of each author

D.S.: data analysis and writing manuscript; T.T., H.E.T.B., E.V., J.S.: data generation and analysis; S.Y.C., M.R.: data analysis and writing manuscript; and R.L.: experimental design, interpretation of data, and writing manuscript. All authors: final approval of the manuscript.

### Conflict of interest

S.Y.C. has served as a consultant for Zogenix, Vivus, Aerpio, and United Therapeutics; S.Y.C. is a director, officer, and shareholder in Numa Therapeutics; S.Y.C. holds research grants from Actelion and Pfizer. S.Y.C. has filed patent applications regarding the targeting of metabolism in pulmonary hypertension. R.L. has served as a consultant for Bristol-Myers Squibb, Boehringer Mannheim, Merck, and Genentech/Roche, and holds research grants from Formation, Elpidera, and Kiniksa.

### Funding

This work was supported by NIH grants: 2P50 AR060780 (R.L.) and R01 HL124021, HL122596, HL138437, and UH2 TR002073, as well as the AHA grant 18EIA33900027 (S.Y.C.).

### ORCID iD

Didem Saygin  <https://orcid.org/0000-0003-1675-597X>

### References

1. Mehta S and Shoemaker GJ. Improving survival in idiopathic pulmonary arterial hypertension: revisiting the “kingdom of the near-dead”. *Thorax* 2005; 60: 981–983.
2. Farber HW, Miller DP, Poms AD, et al. Five-year outcomes of patients enrolled in the REVEAL registry. *Chest* 2015; 148: 1043–1054.
3. Gao Y, Chen T and Raj JU. Endothelial and smooth muscle cell interactions in the pathobiology of pulmonary hypertension. *Am J Respir Cell Mol Biol* 2016; 54: 451–460.
4. Hemnes AR and Humbert M. Pathobiology of pulmonary arterial hypertension: understanding the roads less travelled. *Eur Respir Rev* 2017; 26: pii: 170093.
5. Tuder RM, Archer SL, Dorfmueller P, et al. Relevant issues in the pathology and pathobiology of pulmonary hypertension. *Turk Kardiyol Dern Ars* 2014; 42: 5–16.
6. Stenmark KR, Frid M and Perros F. Endothelial-to-mesenchymal transition: an evolving paradigm and a promising therapeutic target in PAH. *Circulation* 2016; 133: 1734–1737.
7. Simonneau G, Gatzoulis MA, Adatia I, et al. Updated clinical classification of pulmonary hypertension. *J Am Coll Cardiol* 2013; 62: D34–D41.
8. Simonneau G, Montani D, Celermajer DS, et al. Haemodynamic definitions and updated clinical classification of pulmonary hypertension. *Eur Respir J* 2019; 53: pii: 1801913.
9. Morse C, Tabib T, Sembrat J, et al. Proliferating SPP1/MERTK-expressing macrophages in idiopathic pulmonary fibrosis. *Eur Respir J* 2019; 54: pii: 1802441.

10. Satija R, Farrell JA, Gennert D, et al. Spatial reconstruction of single-cell gene expression data. *Nat Biotechnol* 2015; 33: 495–502.
11. Aibar S, Gonzalez-Blas CB, Moerman T, et al. SCENIC: single-cell regulatory network inference and clustering. *Nat Methods* 2017; 14: 1083–1086.
12. Tabib T, Morse C, Wang T, et al. SFRP2/DPP4 and FMO1/LSP1 define major fibroblast populations in human skin. *J Invest Dermatol* 2018; 138: 802–810.
13. Valenzi E, Bulik M, Tabib T, et al. Single-cell analysis reveals fibroblast heterogeneity and myofibroblasts in systemic sclerosis-associated interstitial lung disease. *Ann Rheum Dis* 2019; 78: 1379–1387.
14. Paquet-Fifield S, Schluter H, Li A, et al. A role for pericytes as microenvironmental regulators of human skin tissue regeneration. *J Clin Invest* 2009; 119: 2795–2806.
15. Zhang H, Wang D, Li M, et al. Metabolic and proliferative state of vascular adventitial fibroblasts in pulmonary hypertension is regulated through a microRNA-124/PTBP1 (polypyrimidine tract binding protein 1)/pyruvate kinase muscle axis. *Circulation* 2017; 136: 2468–2485.
16. Stearman RS, Bui QM, Speyer G, et al. Systems analysis of the human pulmonary arterial hypertension lung transcriptome. *Am J Respir Cell Mol Biol* 2019; 60: 637–649.
17. Fernandez RA, Wan J, Song S, et al. Upregulated expression of STIM2, TRPC6, and Orai2 contributes to the transition of pulmonary arterial smooth muscle cells from a contractile to proliferative phenotype. *Am J Physiol Cell Physiol* 2015; 308: C581–C593.
18. Pousada G, Balloira A, Fontan D, et al. Mutational and clinical analysis of the ENG gene in patients with pulmonary arterial hypertension. *BMC Genet* 2016; 17: 72.
19. Hirose S, Hosoda Y, Furuya S, et al. Expression of vascular endothelial growth factor and its receptors correlates closely with formation of the plexiform lesion in human pulmonary hypertension. *Pathol Int* 2000; 50: 472–479.
20. Perros F, Montani D, Dorfmueller P, et al. Platelet-derived growth factor expression and function in idiopathic pulmonary arterial hypertension. *Am J Respir Crit Care Med* 2008; 178: 81–88.
21. Izikki M, Guignabert C, Fadel E, et al. Endothelial-derived FGF2 contributes to the progression of pulmonary hypertension in humans and rodents. *J Clin Invest* 2009; 119: 512–523.
22. Vadapalli S, Rani HS, Sastry B, et al. Endothelin-1 and endothelial nitric oxide polymorphisms in idiopathic pulmonary arterial hypertension. *Int J Mol Epidemiol Genet* 2010; 1: 208–213.
23. Dabral S, Tian X, Kojonazarov B, et al. Notch1 signalling regulates endothelial proliferation and apoptosis in pulmonary arterial hypertension. *Eur Respir J* 2016; 48: 1137–1149.
24. Kim J, Kang Y, Kojima Y, et al. An endothelial apelin-FGF link mediated by miR-424 and miR-503 is disrupted in pulmonary arterial hypertension. *Nat Med* 2013; 19: 74–82.
25. Tatemoto K, Hosoya M, Habata Y, et al. Isolation and characterization of a novel endogenous peptide ligand for the human APJ receptor. *Biochem Biophys Res Commun* 1998; 251: 471–476.
26. Jia YX, Lu ZF, Zhang J, et al. Apelin activates L-arginine/nitric oxide synthase/nitric oxide pathway in rat aortas. *Peptides* 2007; 28: 2023–2029.
27. Kehoe K, Van Elzen R, Verkerk R, et al. Prolyl carboxypeptidase purified from human placenta: its characterization and identification as an apelin-cleaving enzyme. *Biochim Biophys Acta* 2016; 1864: 1481–1488.
28. Adams GN, Stavrou EX, Fang C, et al. Prolylcarboxypeptidase promotes angiogenesis and vascular repair. *Blood* 2013; 122: 1522–1531.
29. Cottin V, Dupuis-Girod S, Lesca G, et al. Pulmonary vascular manifestations of hereditary hemorrhagic telangiectasia (rendu-osler disease). *Respiration* 2007; 74: 361–378.
30. Gore B, Izikki M, Mercier O, et al. Key role of the endothelial TGF-beta/ALK1/endothelin signaling pathway in humans and rodents pulmonary hypertension. *PLoS One* 2014; 9: e100310.
31. Voelkel NF and Gomez-Arroyo J. The role of vascular endothelial growth factor in pulmonary arterial hypertension. The angiogenesis paradox. *Am J Respir Cell Mol Biol* 2014; 51: 474–484.
32. Atkinson C, Stewart S, Upton PD, et al. Primary pulmonary hypertension is associated with reduced pulmonary vascular expression of type II bone morphogenetic protein receptor. *Circulation* 2002; 105: 1672–1678.
33. Dai C, Gong Q, Cheng Y, et al. Regulatory mechanisms of Robo4 and their effects on angiogenesis. *Biosci Rep* 2019; 39: pii: BSR20190513.
34. Jones CA, London NR, Chen H, et al. Robo4 stabilizes the vascular network by inhibiting pathologic angiogenesis and endothelial hyperpermeability. *Nat Med* 2008; 14: 448–453.
35. Mazzoni J, Smith JR, Shahriar S, et al. The Wnt inhibitor Apcdd1 coordinates vascular remodeling and barrier maturation of retinal blood vessels. *Neuron* 2017; 96: 1055–1069 e1056.
36. Hu Z, Wang C, Xiao Y, et al. NDST1-dependent heparan sulfate regulates BMP signaling and internalization in lung development. *J Cell Sci* 2009; 122: 1145–1154.
37. Colladel R, Pellicani R, Andreuzzi E, et al. MULTIMERIN2 binds VEGF-A primarily via the carbohydrate chains exerting an angiostatic function and impairing tumor growth. *Oncotarget* 2016; 7: 2022–2037.
38. Lorenzon E, Colladel R, Andreuzzi E, et al. MULTIMERIN2 impairs tumor angiogenesis and growth by interfering with VEGF-A/VEGFR2 pathway. *Oncogene* 2012; 31: 3136–3147.
39. MacKenzie F, Duriez P, Wong F, et al. Notch4 inhibits endothelial apoptosis via RBP-Jkappa-dependent and -independent pathways. *J Biol Chem* 2004; 279: 11657–11663.
40. Carlson TR, Yan Y, Wu X, et al. Endothelial expression of constitutively active Notch4 elicits reversible arteriovenous malformations in adult mice. *Proc Natl Acad Sci USA* 2005; 102: 9884–9889.
41. Lehman A, Wuyts W and Patel MS. Adams–Oliver syndrome. In: Adam MP, Ardinger HH, Pagon RA, et al. (eds) *GeneReviews((R))*. Seattle, WA: University of Washington, 1993.
42. Stittrich AB, Lehman A, Bodian DL, et al. Mutations in NOTCH1 cause Adams–Oliver syndrome. *Am J Hum Genet* 2014; 95: 275–284.
43. Sukalo M, Tilsen F, Kayserili H, et al. DOCK6 mutations are responsible for a distinct autosomal-recessive variant of Adams–Oliver syndrome associated with brain and eye anomalies. *Hum Mutat* 2015; 36: 1112.

44. Cermenati S, Moleri S, Cimbro S, et al. Sox18 and Sox7 play redundant roles in vascular development. *Blood* 2008; 111: 2657–2666.
45. Downes M and Koopman P. SOX18 and the transcriptional regulation of blood vessel development. *Trends Cardiovasc Med* 2001; 11: 318–324.
46. Fontijn RD, Favre J, Naaijken BA, et al. Adipose tissue-derived stromal cells acquire endothelial-like features upon reprogramming with SOX18. *Stem Cell Res* 2014; 13: 367–378.
47. Gross CM, Aggarwal S, Kumar S, et al. Sox18 preserves the pulmonary endothelial barrier under conditions of increased shear stress. *J Cell Physiol* 2014; 229: 1802–1816.
48. Chakrabarti J, Turley H, Campo L, et al. The transcription factor DEC1 (stra13, SHARP2) is associated with the hypoxic response and high tumour grade in human breast cancers. *Br J Cancer* 2004; 91: 954–958.
49. Ivanov SV, Sahnikow K, Ivanova AV, et al. Hypoxic repression of STAT1 and its downstream genes by a pVHL/HIF-1 target DEC1/STRA13. *Oncogene* 2007; 26: 802–812.
50. Ivanova AV, Ivanov SV, Zhang X, et al. STRA13 interacts with STAT3 and modulates transcription of STAT3-dependent targets. *J Mol Biol* 2004; 340: 641–653.
51. Pirot N, Deleuze V, El-Hajj R, et al. LYL1 activity is required for the maturation of newly formed blood vessels in adulthood. *Blood* 2010; 115: 5270–5279.
52. Deleuze V, El-Hajj R, Chalhoub E, et al. Angiopoietin-2 is a direct transcriptional target of TAL1, LYL1 and LMO2 in endothelial cells. *PLoS One* 2012; 7: e40484.
53. Gross C, Buchwalter G, Dubois-Pot H, et al. The ternary complex factor net is downregulated by hypoxia and regulates hypoxia-responsive genes. *Mol Cell Biol* 2007; 27: 4133–4141.
54. Gross C, Dubois-Pot H and Wasylyk B. The ternary complex factor Net/Elk-3 participates in the transcriptional response to hypoxia and regulates HIF-1 alpha. *Oncogene* 2008; 27: 1333–1341.
55. Zheng H, Wasylyk C, Ayadi A, et al. The transcription factor Net regulates the angiogenic switch. *Genes Dev* 2003; 17: 2283–2297.
56. Holmberg C, Helin K, Sehested M, et al. E2F-1-induced p53-independent apoptosis in transgenic mice. *Oncogene* 1998; 17: 143–155.
57. Loughran O and La Thangue NB. Apoptotic and growth-promoting activity of E2F modulated by MDM2. *Mol Cell Biol* 2000; 20: 2186–2197.
58. Pajalunga D, Tognozzi D, Tiainen M, et al. E2F activates late-G1 events but cannot replace E1A in inducing S phase in terminally differentiated skeletal muscle cells. *Oncogene* 1999; 18: 5054–5062.
59. Strom DK, Cleveland JL, Chellappan S, et al. E2F-1 and E2F-3 are functionally distinct in their ability to promote myeloid cell cycle progression and block granulocyte differentiation. *Cell Growth Differ* 1998; 9: 59–69.
60. Spyridopoulos I, Principe N, Krasinski KL, et al. Restoration of E2F expression rescues vascular endothelial cells from tumor necrosis factor-alpha-induced apoptosis. *Circulation* 1998; 98: 2883–2890.
61. Tiana M, Acosta-Iborra B, Puente-Santamaria L, et al. The SIN3A histone deacetylase complex is required for a complete transcriptional response to hypoxia. *Nucleic Acids Res* 2018; 46: 120–133.
62. Biddlestone J, Batie M, Bandarra D, et al. SINHCAF/FAM60A and SIN3A specifically repress HIF-2alpha expression. *Biochem J* 2018; 475: 2073–2090.
63. Chang S, Young BD, Li S, et al. Histone deacetylase 7 maintains vascular integrity by repressing matrix metalloproteinase 10. *Cell* 2006; 126: 321–334.
64. Mottet D, Bellahcene A, Pirotte S, et al. Histone deacetylase 7 silencing alters endothelial cell migration, a key step in angiogenesis. *Circ Res* 2007; 101: 1237–1246.
65. Turtoi A, Mottet D, Matheus N, et al. The angiogenesis suppressor gene AKAP12 is under the epigenetic control of HDAC7 in endothelial cells. *Angiogenesis* 2012; 15: 543–554.
66. Ha CH, Jhun BS, Kao HY, et al. VEGF stimulates HDAC7 phosphorylation and cytoplasmic accumulation modulating matrix metalloproteinase expression and angiogenesis. *Arterioscler Thromb Vasc Biol* 2008; 28: 1782–1788.
67. Boise LH, Gonzalez-Garcia M, Postema CE, et al. bcl-x, a bcl-2-related gene that functions as a dominant regulator of apoptotic cell death. *Cell* 1993; 74: 597–608.
68. Wang L, Wang P, Dong H, et al. Ulk1/FUNDC1 prevents nerve cells from hypoxia-induced apoptosis by promoting cell autophagy. *Neurochem Res* 2018; 43: 1539–1548.
69. Sekine Y, Hatanaka R, Watanabe T, et al. The Kelch repeat protein KLHDC10 regulates oxidative stress-induced ASK1 activation by suppressing PP5. *Mol Cell* 2012; 48: 692–704.
70. Mori S, Araki M, Ishii S, et al. LPA signaling through LPA receptors regulates cellular functions of endothelial cells treated with anticancer drugs. *Mol Cell Biochem* 2015; 408: 147–154.
71. Nguyen TH, Bertrand MJ, Sterpin C, et al. Maged1, a new regulator of skeletal myogenic differentiation and muscle regeneration. *BMC Cell Biol* 2010; 11: 57.
72. Yan X, Wang J, Zhu Y, et al. S1P induces pulmonary artery smooth muscle cell proliferation by activating calcineurin/NFAT/OPN signaling pathway. *Biochem Biophys Res Commun* 2019; 516: 921–927.
73. Bjerke GA, Hyman-Walsh C and Wotton D. Cooperative transcriptional activation by Klf4, Meis2, and Pbx1. *Mol Cell Biol* 2011; 31: 3723–3733.
74. Pliner HA, Packer JS, McFaline-Figueroa JL, et al. Cicero predicts cis-regulatory DNA interactions from single-cell chromatin accessibility data. *Mol Cell* 2018; 71: 858–871 e858.
75. McCulley DJ, Wienhold MD, Hines EA, et al. PBX transcription factors drive pulmonary vascular adaptation to birth. *J Clin Invest* 2018; 128: 655–667.
76. Huang Q, Zhang L, Wang Y, et al. Depletion of PHF14, a novel histone-binding protein gene, causes neonatal lethality in mice due to respiratory failure. *Acta Biochim Biophys Sin (Shanghai)* 2013; 45: 622–633.
77. Schinagl C, Melum GR, Rodningen OK, et al. Severe persistent pulmonary hypertension of the newborn and dysmorphic features in neonate with a deletion involving TWIST1 and PHF14: a case report. *J Med Case Rep* 2017; 11: 226.
78. Hong EA, Gautrey HL, Elliott DJ, et al. SAFB1- and SAFB2-mediated transcriptional repression: relevance to cancer. *Biochem Soc Trans* 2012; 40: 826–830.
79. Sakhneny L, Rachi E, Epshtein A, et al. Pancreatic pericytes support beta-cell function in a Tcf7l2-dependent manner. *Diabetes* 2018; 67: 437–447.

80. O'Reilly MS, Boehm T, Shing Y, et al. Endostatin: an endogenous inhibitor of angiogenesis and tumor growth. *Cell* 1997; 88: 277–285.
81. Zhang B, Dietrich UM, Geng JG, et al. Repulsive axon guidance molecule Slit3 is a novel angiogenic factor. *Blood* 2009; 114: 4300–4309.
82. Fujiwara H, Ferreira M, Donati G, et al. The basement membrane of hair follicle stem cells is a muscle cell niche. *Cell* 2011; 144: 577–589.
83. Amsellem V, Lipskaia L, Abid S, et al. CCR5 as a treatment target in pulmonary arterial hypertension. *Circulation* 2014; 130: 880–891.
84. Florentin J, Coppin E, Vasamsetti SB, et al. Inflammatory macrophage expansion in pulmonary hypertension depends upon mobilization of blood-borne monocytes. *J Immunol* 2018; 200: 3612–3625.
85. Frid MG, Brunetti JA, Burke DL, et al. Circulating mononuclear cells with a dual, macrophage-fibroblast phenotype contribute robustly to hypoxia-induced pulmonary adventitial remodeling. *Chest* 2005; 128: 583S–584S.
86. Sartina E, Suguihara C, Ramchandran S, et al. Antagonism of CXCR7 attenuates chronic hypoxia-induced pulmonary hypertension. *Pediatr Res* 2012; 71: 682–688.
87. Hiramoto Y, Shioyama W, Higuchi K, et al. Clinical significance of plasma endothelin-1 level after bosentan administration in pulmonary arterial hypertension. *J Cardiol* 2009; 53: 374–380.